Linear stability analysis of convective chemical fronts in a vertical slab

Desiderio A. Vasquez and Casey Lengacher
Department of Physics, Indiana University–Purdue University Fort Wayne, Fort Wayne, Indiana 46805-1499
(Received 4 March 1998)

A chemical reaction front propagating in a viscous fluid separates two liquids of different densities leading to convection. Convection enhances the speed and changes the curvature of the front. We analyze the effects of convection as the front propagates in a two-dimensional vertical slab. In this geometry, the fluid motion can be described using Brinkman's equations [Appl. Sci. Res., Sect. A **1**, 27 (1947)]. This set of equations is coupled to a front evolution equation describing the motion of the convective chemical front. Convection will be present depending on the slab width and gap thickness. The steady state solutions can be axisymmetric or nonaxisymmetric fronts depending on the slab width. A linear stability analysis for the solutions shows a region of bistability for narrow gaps. The bistability disappears as the slab width is increased.
[S1063-651X(98)09711-6]

PACS number(s): 47.20.Bp, 47.70.Fw, 03.40.Gc

I. INTRODUCTION

Experiments have shown that convective fluid motion significantly alters the behavior of chemical fronts and waves. Miike *et al.* have observed that the chemical waves in the Belousov-Zhabotinskii reaction are coupled to convective rolls as they travel in a thin layer of liquid [1]. Experiments by Pojman and co-workers have shown the complex behavior of chemical waves in the bromate-sulfite system [2] as well as double-diffusive convection in the iodate-sulfite system [3]. Martincigh, Hauser, and Simoyi identified thermal plumes due to convection caused by an exothermic autocatalytic reaction [4]. Masere *et al.* [5] obtained axisymmetric and nonaxisymmetric fronts in the iodate-arsernous acid reaction in vertical cylinders. In this system, convection is caused mainly by the density difference between reacted and unreacted fluid. Carey *et al.* [6] used this reaction for experiments in a two-dimensional vertical slab.

Previous theoretical work treated the convective chemical front using two models for front propagation: a reaction-diffusion model [7] and a front evolution model similar to the Kuramoto-Sivashinskii equation for flame propagation [8]. Each of these models was applied to two different geometries: a vertical cylinder [9] and a vertical slab [10]. In the vertical cylinder the convectionless front loses stability to either axisymmetric or nonaxisymmetric convection depending on the diameter of the cylinder [9]. This theoretical result based on the front evolution model was later confirmed by the experiments [5]. The studies in the vertical slab also show axisymmetric and nonaxisymmetric convection [11]. However, the models based on the front evolution equation did not yield stable axisymmetric fronts [12], whereas the models based on the reaction-diffusion equations did show stable axisymmetric fronts [13]. These results are even more intriguing if the Navier-Stokes equations are replaced with Darcy's law in the narrow gap limit. In this limit, an axisymmetric front becomes stable even with the front evolution model [14]. A linear stability analysis using the front evolution model in both cases (the Navier-Stokes equations and Darcy's law) showed bistability between axisymmetric and nonaxisymmetric fronts with Darcy's law, but only unstable axisymmetric fronts for the Navier-Stokes equations [14]. In this paper we show how the front stability changes as the gap thickness increases using an approximation valid for wider gaps: Brinkman's equations [15]. Recent calculations using Brinkman's equations show important finite-gap corrections to double-diffusive systems in a vertical slab [16]. The advantage of Brinkman's equations is that they reduce to Darcy's law and the Navier-Stokes equations in the appropriate limits. In this paper we carry out a linear stability analysis of convective chemical fronts in vertical slabs using Brinkman's equations. Our results will show a region of bistability between axisymmetric and nonaxisymmetric fronts for narrow gaps. This bistability is not present for wider gaps.

II. EQUATIONS OF MOTION

Chemical fronts in the iodate-arsenous equation can be described [14] with a nonlinear front evolution equation for small curvatures:

$$\frac{\partial H}{\partial t} = D\frac{\partial^2 H}{\partial x^2} + \frac{c_0}{2}\left(\frac{\partial H}{\partial x}\right)^2 + V_z|_{z=H}. \tag{1}$$

Here $H(x,t)$ indicates the front height in the vertical z direction, c_0 is the flat front speed, and $V_z|_{z=H}$ is the vertical component of the fluid flow at the front. The horizontal direction is along the x axis. The front height is measured from a reference frame comoving with the front. The solution $H=0$ corresponds to the flat front moving at constant speed in the laboratory frame. This equation was obtained from a reaction-diffusion model coupled to the corresponding hydrodynamic equations. To model the fluid flow in a vertical slab, we use the linearized Brinkman equations in a reference frame moving with the flat front speed c_0:

$$\omega = \nabla^2 \psi \tag{2}$$

and

$$\frac{\partial \omega}{\partial t} = \nu\nabla^2\omega - \frac{12\nu}{a^2}\omega + g\frac{\partial \delta\rho}{\partial x} + c_0\frac{\partial \omega}{\partial z}. \tag{3}$$

Here ω is the vorticity, $\delta\rho$ is the fractional change in density across the front, g is the acceleration of gravity, a is the gap thickness, and ν is the kinematic viscosity. The stream function ψ relates to the components of the fluid velocity by $V_x = \partial\psi/\partial z$ and $V_z = -\partial\psi/\partial x$. The density difference changes abruptly at the front; this change leads to jump conditions for the stream function

$$[\psi] = \left[\frac{\partial\psi}{\partial x}\right] = \left[\frac{\partial^2\psi}{\partial x^2}\right] = 0 \tag{4}$$

and

$$\left[\frac{\partial^3\psi}{\partial x^3}\right] = \frac{g\delta_0}{\nu}\frac{\partial H}{\partial x}. \tag{5}$$

Here δ_0 indicates the fractional density difference between reacted and unreacted fluid. The terms in square brackets indicate the value of any function in the unreacted side of the front minus the value in the reacted side of the front. A previous analysis [14] showed that the terms in square brackets can be evaluated at $H=0$ for this front evolution approximation. These equations are solved using a Fourier expansion on the front height:

$$H(x,t) = \sum_n H_n(t)\cos(nqx). \tag{6}$$

The number q is determined by the slab width b, with $q = \pi/b$. It corresponds to the wave number q for perturbations on an unbounded front [10]. We chose free boundary conditions on the horizontal direction. This facilitates a comparison with the narrow gap limit (where Darcy's law is valid) because this limit only requires no fluid flow in the normal direction. This also helps to compare with previous calculations based on the Navier-Stokes equations with free boundary conditions. This will show that the differences and similarities between both limits are due to the type of approximation for the fluid flow and not to the boundary conditions. It also makes the fluid equations separable with a considerable simplification in the calculations. Relating the vertical component of the velocity to a Fourier expansion on the stream function as in [14], we obtain the front evolution that involves only the front height and its Fourier coefficients:

$$\frac{\partial H}{\partial t} = D\frac{\partial^2 H}{\partial x^2} + \frac{c_0}{2}\left(\frac{\partial H}{\partial x}\right)^2 + \frac{g\delta_0}{2\nu}\sum_n \frac{(nq)H_n\cos(nqx)}{[nq+\sqrt{(nq)^2+k}][\sqrt{(nq)^2+k}]}. \tag{7}$$

Here the parameter k is related to the gap thickness by $k = 12/a^2$. At this point we introduce dimensionless units for the length $(D\nu/g\delta_0)^{1/3}$, the time $(Dg^2\delta_0^2/\nu^2)^{-1/3}$, and the front height D/c_0. We finally obtain a set of ordinary differential equations for the Fourier coefficients of the front height:

$$\frac{dH_0}{dt} = \frac{q^2}{4}\sum_{n=1} n^2 H_n^2 \tag{8}$$

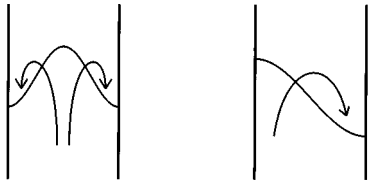

FIG. 1. Descriptive sketch indicating the two types of convective fronts. Nonaxisymmetric fronts involve a single convective roll, where axisymmetric solutions involve two rolls.

and

$$\frac{dH_p}{dt} = \left(-p^2q^2 + \frac{pq}{2[pq+\sqrt{(pq)^2+\chi}][\sqrt{(pq)^2+\chi}]}\right)H_p + \frac{q^2}{4}\sum_{n=1}\sum_{m=1} nmH_nH_m(\delta_{p,n-m}+\delta_{p,n+m}) \quad \text{for } p \geqslant 1. \tag{9}$$

Here $\chi = (D\nu/g\delta_0)^{2/3}(12/a^2)$ is the only parameter that depends on a, the gap thickness.

Important features of the convective fronts can be studied with a two-variable model. We obtain this model by keeping four terms in the expansion [Eq. (9)] while setting the time derivatives for the last two terms to zero. The model is further simplified by including only third-order terms, which result in

$$\frac{dH_1}{dt} = [-q^2 + f(q)]H_1 + q^2H_1H_2 - \frac{3q^4}{[9q^2 - f(3q)]}H_1H_2^2 \tag{10}$$

and

$$\frac{dH_2}{dt} = [-4q^2 + f(2q)]H_2 - \frac{q^2}{4}H_1^2 - \frac{4q^4}{[16q^2 - f(4q)]}H_2^3 - \frac{3q^4}{2[9q^2 - f(3q)]}H_1^2H_2. \tag{11}$$

The function f is defined as

$$f(x) = \frac{x}{2(x+\sqrt{q^2+\chi})(\sqrt{q^2+\chi})}. \tag{12}$$

III. RESULTS

The solutions of the two-variable model are flat, axisymmetric, and nonaxisymmetric fronts. Flat fronts are convectionless, where curved fronts involve steady convection as shown in Fig. 1. We obtained these solutions analytically. The flat fronts ($H_1 = H_2 = 0$) are unstable for small values of q, which correspond to large slab widths b. The stability analysis of the flat front with free boundaries is equivalent to the analysis of the unbounded front, which was carried out elsewhere [10]. This study showed that flat fronts are unstable for perturbations of wave numbers below a critical wave number q_c, with q_c depending on the gap thickness,

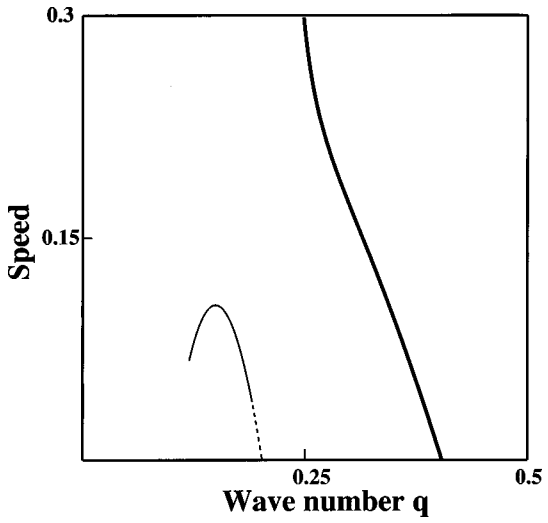

FIG. 2. Speed of the fronts as a function of wave number q for the two-variable model. The bold line indicates stable nonaxisymmetric fronts. The thin lines indicate axisymmetric fronts. The broken line indicates that the front is unstable. The speed is measured relative to the flat front speed. The units are the dimensionless units defined in the paper.

which in turn determines χ. Nonaxisymmetric fronts appear for wave numbers below q_c as shown in Fig. 2 for $\chi=0.7$. An analytical solution of the two-variable model shows that the speed of these fronts is enhanced by convection. Axisymmetric solutions are allowed for wave numbers below $q_c/2$. A linear stability analysis showed that the nonaxisymmetric fronts are always stable, where the axisymmetric fronts are unstable near $q_c/2$, but become stable for lower values [14].

Numerical solutions of Eqs. (8) and (9) using 100 variables H_p are summarized in Fig. 3 for $\chi=0.7$. As with the

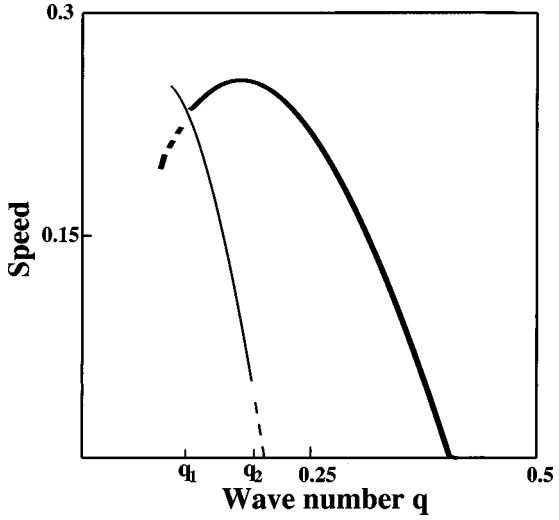

FIG. 3. Speed of the fronts as a function of wave number q using 100 terms in the Fourier expansion. The bold and thin lines indicates nonaxisymmetric and axisymmetric fronts, respectively. The broken lines indicate that the corresponding front is unstable. The wave numbers q_1 and q_2 indicate the change of stability for nonaxisymmetric and axisymmetric fronts, respectively. The speed is measured relative to the flat front speed. The units are the dimensionless units defined in the paper.

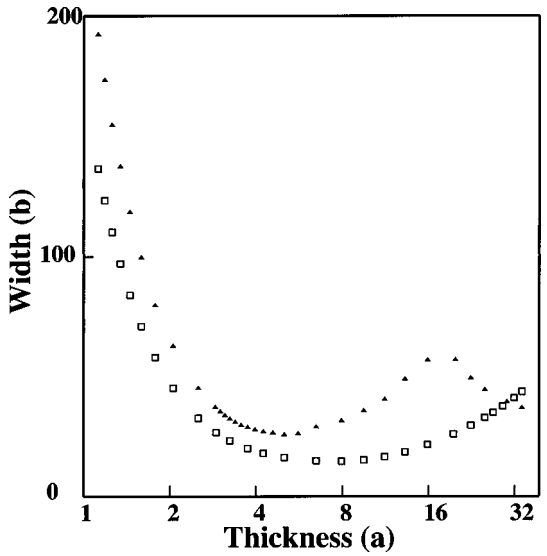

FIG. 4. Region of bistability of axisymmetric and nonaxisymmetric fronts. For widths below the triangles we find stable nonaxisymmetric fronts. For widths above the squares we find stable axisymmetric fronts. For slab widths below the triangles and above the squares both types of fronts can coexist, thus defining a region of bistability for gap thicknesses below $a=30.4$.

two-variable model the solutions can be flat, axisymmetric, or nonaxisymmetric. Both models show nonaxisymmetric solutions for values below q_c and axisymmetric solutions below $q_c/2$. In both cases the axisymmetric solutions are unstable near $q_c/2$, becoming stable for lower values. However, the results are significantly different in other respects. In the two-variable model, the speed of the nonaxisymmetric front becomes unlimited, where in the large term expansion, the speed of the axisymmetric front reaches a maximum value. The large term expansion also shows that the nonaxisymmetric front becomes unstable for values of q below a critical number q_2. The axisymmetric fronts are unstable near $q_c/2$, but become stable for values below q_1, as shown in Fig. 3. There is a region of bistability where nonaxisymmetric and axisymmetric fronts are stable. This region is for q between q_1 and q_2. This bistability was also reported for flow in porous media in [14]. We have to report an erratum in Fig. 5 of that reference (which is analogous to our Fig. 3) where the front speed is off by a factor of 4. The speeds in that figure have to be divided by 4. This erratum does not change any of the conclusions or the region of bistability. The values of q_1 and q_2 determine two values for the slab width b_1 and b_2, with $b_{1,2}=\pi/q_{1,2}$. Based on the previous discussion, there is bistability for slab widths b with $b_1<b<b_2$. In Fig. 4 we show the values of b_1 and b_2 as a function of the gap thickness. We found that for small gap thicknesses b_2 remains larger than b_1, which indicates that the region of bistability exists. For gap thicknesses larger than 30.4, we find that b_1 goes above b_2, indicating no bistability. This result is consistent with a previous calculation that found no bistability for Navier-Stokes flow and bistability for flow governed by Darcy's law. The Navier-Stokes equations are the limit for Brinkman's equations for large gap separation, whereas Darcy's law is the limit for small gaps. Since the value of χ has to be small for the bistability to disappear, we expect that the bistability will be present in

experiments, although the precise regions of bistability may be different due to the use of free boundary conditions. We expect that the theory will be particularly useful near the transition from flat to nonaxisymmetric fronts since in this region the fronts have small curvature. For large curvatures, the front evolution equation will have to be replaced with the full eikonal relation [17] or with a reaction-diffusion model [18].

IV. CONCLUSION

In summary, we found axisymmetric and nonaxisymmetric fronts in vertical slabs. The linear stability analysis showed that the nonaxisymmetric fronts are stable near the onset of convection, whereas the axisymmetric fronts become stable away from onset. For small gaps, there is a region of bistability between both types of convective fronts. Our calculations are consistent with previous results for viscous fluids (large gap limit) and for flow in porous media (small gap limit).

ACKNOWLEDGMENT

This research was supported by a grant from the Research Corporation.

[1] H. Miike, S. C. Muller, and B. Hess, Phys. Lett. A **141**, 25 (1989).
[2] J. A. Pojman, I. P. Nagy, and A. Keresztessy, J. Phys. Chem. **99**, 5385 (1995).
[3] J. A. Pojman, A. Komlosi, and I. P. Nagy, J. Phys. Chem. **100**, 16 209 (1996).
[4] B. S. Martincigh, M. J. B. Hauser, and R. H. Simoyi, Phys. Rev. E **52**, 6146 (1996).
[5] J. Masere, D. A. Vasquez, B. F. Edwards, J. W. Wilder, and K. Showater, J. Phys. Chem. **98**, 6505 (1994).
[6] M. R. Carey, S. W. Morris, and P. Kolodner, Phys. Rev. E **53**, 6012 (1996).
[7] D. A. Vasquez, J. M. Littley, J. W. Wilder, and B. F. Edwards, Phys. Rev. E **50**, 280 (1994).
[8] J. W. Wilder, D. A. Vasquez, B. F. Edwards, and G. I. Sivashinsky, Physica D **73**, 217 (1994).
[9] D. A. Vasquez, J. W. Wilder, and B. F. Edwards, Phys. Fluids A **4**, 2410 (1992).
[10] J. Huang, D. A. Vasquez, B. F. Edwards, and P. Kolodner, Phys. Rev. E **48**, 4378 (1993).
[11] D. A. Vasquez, B. F. Edwards, and J. W. Wilder, Phys. Rev. A **43**, 6694 (1991).
[12] J. W. Wilder, D. A. Vasquez, and B. F. Edwards, Physica D **90**, 170 (1996).
[13] Y. Wu, D. A. Vasquez, J. W. Wilder, and B. F. Edwards, Phys. Rev. E **52**, 6175 (1995).
[14] D. A. Vasquez, Phys. Rev. E **56**, 6767 (1997).
[15] H. C. Brinkman, Appl. Sci. Res., Sect. A **1**, 27 (1947).
[16] A. A. Predtechensky, W. D. McCormick, J. B. Swift, A. G. Rossberg, and H. L. Swinney, Phys. Fluids **6**, 3923 (1994).
[17] B. F. Edwards, J. W. Wilder, and K. Showalter, Phys. Rev. A **43**, 749 (1991).
[18] D. A. Vasquez, J. W. Wilder, and B. F. Edwards, J. Phys. Chem. **104**, 9926 (1996).